สัมมนาวิชาการวิศวกรรมเครื่องกลแห่งประเทศไทยครั้งที่ 13
2-3 ธันวาคม 2542 โรงแรม รอยัลคลิฟบีชรีสอร์ท พัทยาใต้ ชลบุรี

การประเมินขั้นตอนวิธีสำหรับการสร้างรูปร่างของคุณสมบัติเปลวเพลิงเทอร์บิวเลนท์โดยวิธีโทโมกราฟฟีแบบไม่ต่อเนื่องด้วยข้อมูลจำกัด

Evaluation of An Algorithm for Discrete Tomographic Reconstruction of Turbulent Flame-property Profiles from Limited Data

พงศาล มีคุณสมบัติ, จีระวรรณ เกตุนุ้ย, ปูมยศ วัลลิกุล, บัณฑิต ฟุ้งธรรมสาร
ศูนย์วิจัยการเผากากของเสีย ภาควิชาวิศวกรรมเครื่องกล คณะวิศวกรรมศาสตร์
สถาบันเทคโนโลยีพระจอมเกล้าพระนครเหนือ กรุงเทพฯ

Phongsan Meekunnasombat, Jeerawan Ketnuy, Pumyos Vallikul and Bundit Fungtammasan
The Waste Incineration Research Center (WIRC)
Department of Mechanical Engineering
King Mongkut's Institute of Technology North Bangkok

บทคัดย่อ

บทความนี้ได้ศึกษาขั้นตอนวิธีโทโมกราฟฟีแบบไม่ต่อเนื่องในการสร้างภาพเสมือนของรูปร่างคุณสมบัติเปลวเพลิงเทอร์บิวเลนท์จากข้อมูลการดูดกลืนที่จำกัด เปลวเพลิงทดสอบจำลองขึ้นโดยให้มีรูปร่างแบบเกาซ์เซียนเยื้องศูนย์ ใช้แทนสนามของค่าการส่งผ่านเฉลี่ยแบบ 2 มิติ การศึกษาครั้งนี้ได้แนะนำวิธีเชิงตัวเลขในการสังเคราะห์กระบวนการอินทิเกรทแบบแถบซึ่งเป็นผลทำให้ได้เมทริกซ์ภาพฉาย ที่แสดงคุณลักษณะแบบไม่ต่อเนื่องของปัญหา จากนั้นทำการสังเคราะห์ภาพฉาย, สร้างเมทริกซ์พิกเซลธรรมชาติ, หาจำนวนการเก็บข้อมูลแนวขวางและจำนวนมุมที่เหมาะสมสำหรับการสร้างภาพเสมือน ขั้นตอนวิธีการสร้างภาพเสมือนที่ศึกษา เพื่อแก้ปัญหาที่มีตัวแปรมากกว่าสมการ มี 2 วิธี คือวิธีพีชคณิต และวิธีการแยกพิกเซลธรรมชาติ ซึ่งผลการศึกษาแสดงให้เห็นว่าวิธีโทโมกราฟฟีแบบไม่ต่อเนื่องยอมให้สร้างภาพเสมือนจากข้อมูลวิถีรวมที่ไม่สมบูรณ์ และวิธีนี้ทำให้เราสามารถสร้างแบบจำลองของข้อมูลการวัดวิถีรวมแบบไม่ต่อเนื่องได้

Abstract

Discrete tomographic reconstruction algorithms for reconstructing turbulent flame-property profiles from limited absorption data have been studied. The turbulent flame is simulated by an off-center Gaussian profile which represents a two dimensional field of average values of transmittance. This study introduces a numerical technique for synthesizing strip integration resulting in a projection matrix that discretely characterizes the problem. The synthetic projections and a natural pixel matrix are then constructed and the appropriate numbers for angular and lateral sampling are determined. Two reconstruction algorithms for underdetermined problems have been used in this study: The algebraic reconstruction technique (ART) and the natural pixel (NP) decomposition technique. It has been found from this study that the discrete tomographic technique tolerates the incomplete data and the method also allows us to model the path integrated measurement data discretely.

1 Introduction

Reconstructing the local probability density functions (local-PDF) of a thermodynamic property within a turbulent flame from their measured path-integrated probability density functions (path-PDF) has evolved only recently. Beginning in 1996, Nyden et al [1] introduced an algorithm for reconstructing moments of local-PDFs (called local moments) of transmittance within an axisymmetric turbulent flame [2] from their measured and computer simulated path-PDFs. Later, Vallikul et al [3] improved upon the algorithm so that it can retrieve the local-PDFs of transmittance at an arbitrary location within the turbulent flame when the reconstructed local moments are given.

Although the algorithm has been shown satisfactory on the basis of the quality of the reconstruction results, an underlying assumption —that the local-PDFs have to be statistically independent— remains questionable. On the other hand since

the Filter Back-projection (FBP) [4] technique has been used during reconstruction, the algorithm becomes semi-discrete and excessive tomographic data are needed in order to obtain consistent reconstruction results [5]. The assumption that the local-PDFs have to be statistically independent and the fact that the method is not tolerant of incomplete tomographic data are the two main disadvantages of the algorithm.

This study is aimed at overcoming the latter disadvantage. The idea is to replace the FBP technique by the Natural Pixel (NP) technique, then study the effects on the quality of the reconstruction. The Natural Pixel (NP) reconstruction technique [6] has been used for incomplete tomographic data [7] and the technique is sometimes called discrete tomography since all the steps in the reconstruction algorithm are fully discrete. In this study a test function is initially set up (section 2), then, a matrix projecting the test function into discrete strips is constructed and analyzed (section 3). The NP method is reviewed in section 4, in which the effects of the number of pixels, projection strips and view angle on the reconstruction results, is studied. Finally the reconstruction result using the NP method is compared with the FBP and with an algebraic reconstruction technique (ART) [8], the results being shown in section 5.

2 Test Function

An off-centered Gaussian profile has been chosen as the test function, f(x,y) for this study. The function has the form

$$f(x,y) = e^{-c[(x-x_0)^2+(y-y_0)^2]} \tag{1}$$

where the constant c and (x_0, y_0) are set to be 20 and (0.4, 0.0) respectively. A surface plot of the function is shown in Figure 1.

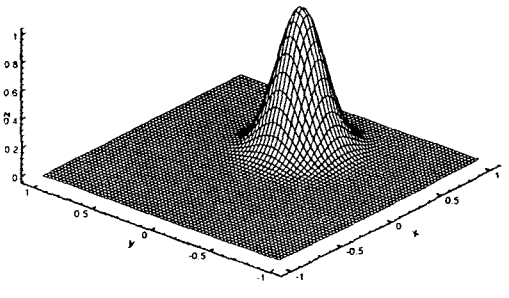

Figure 1 The test function

The off-centered Gaussian profile has the analytical line integrated function at different angles of the form [8]:

$$p_L(r) = \sqrt{\frac{\pi}{c}} e^{-c(r-R)^2} \tag{2}$$

where

$$R = \sqrt{x_0^2 + y_0^2}\cos\left\{\left[\tan^{-1}\left(\frac{y_0}{x_0}\right)\right] - \theta\right\}$$

The line integral (2) will be used, in section 4.2, to calculate the analytical value of projection strips.

3 Construction of the projection matrix

In discrete tomography, the problem is derived in discrete form at the beginning of the reconstruction process. The two-dimensional domain is divided into pXp rectangular pixels and the function, f(x,y), that falls into each pixel, is approximated to have a constant value f_q, (q = 1... p^2), represented by a vector $\underline{f}$. The projection matrix, ϕ, is then defined by the matrix that transforms the vector $\underline{f}$, into the projection vector $\underline{y}$ of length MXN where M and N represent the M view angles and the N number of projections at that view angle. For example, if y_{kn} is the element of vector $\underline{y}$ then y_{kn} represents the value of the n^{th} projection when viewed from the k^{th} angle, hence

$$\phi \underline{f} = \underline{y} \tag{3}$$

The matrix ϕ has MXN rows and p^2 columns, that is,

$$\phi = \begin{bmatrix} \phi_{11,1} & \phi_{11,2} & \cdots & \phi_{11,q} & \cdots & \phi_{11,p^2} \\ \phi_{12,1} & \phi_{12,2} & \cdots & \phi_{12,q} & \cdots & \phi_{12,p^2} \\ \vdots & \vdots & & \vdots & & \vdots \\ \phi_{kn,1} & \phi_{kn,2} & \cdots & \phi_{kn,q} & \cdots & \phi_{kn,p^2} \\ \vdots & \vdots & & \vdots & & \vdots \\ \phi_{MN,1} & \phi_{MN,2} & \cdots & \phi_{MN,q} & \cdots & \phi_{MN,p^2} \end{bmatrix} \tag{4}$$

The vectors $\underline{f}$ and $\underline{y}$ are

$$\underline{f} = \begin{bmatrix} f_1 & f_2 & \cdots & f_q & \cdots & f_{p^2} \end{bmatrix}^T \tag{5}$$

and

$$\underline{y} = \begin{bmatrix} y^T(1) & y^T(2) & \cdots & y^T(k) & \cdots & y^T(M) \end{bmatrix}^T \tag{6}$$

respectively where $y(k) = \begin{bmatrix} y_{k1} & y_{k2} & \cdots & y_{kn} & \cdots & y_{kN} \end{bmatrix}^T$

If the $\underline{y}$ is set to be the strip integral of $\underline{f}$, then each element of $\phi_{kn,q}$ represents a portion of the area of the n^{th} strip of the k^{th} view angle that passes through the pixel q. Calculation of the value of each element of ϕ is a matter of determining the area of a polygon [6].

3.1 Evaluating the projection matrix: a simple example

Consider a domain consisting of 3X3 pixels and let each pixel has an area of unity. Two strips pass the pixels at the view angles of 0° and 90° respectively as shown in Figure 2.

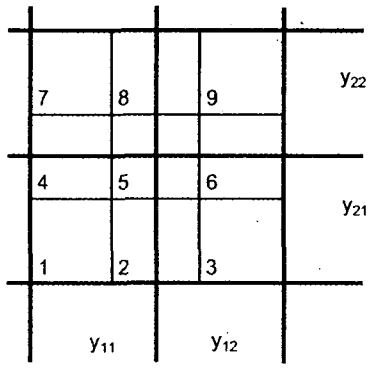

Figure 2 An example of function decomposition uses (3x3 pixels and 4 projection strips).

The matrix ϕ, according to (4), can simply be written as

$$\phi = \begin{bmatrix} 1 & 0.5 & 0 & 1 & 0.5 & 0 & 1 & 0.5 & 0 \\ 0 & 0.5 & 1 & 0 & 0.5 & 1 & 0 & 0.5 & 1 \\ 1 & 1 & 1 & 0.5 & 0.5 & 0.5 & 0 & 0 & 0 \\ 0 & 0 & 0 & 0.5 & 0.5 & 0.5 & 1 & 1 & 1 \end{bmatrix} \qquad (7)$$

4. Natural pixel decomposition reconstruction

Natural pixel decomposition (NP) is a technique for reconstructing a function from its incomplete tomographic data. With this technique, the vector $\underline{f}$ is written as linear combinations of the column space of ϕ^T:

$$\underline{f} = \phi^T \underline{x} \qquad (8)$$

where the elements of $\underline{x}$ are unknown. The vector $\underline{x}$ is

$$\underline{x} = \left[x^T(1) \quad x^T(2) \quad \cdots \quad x^T(k) \quad \cdots \quad x^T(M)\right]^T$$

and

$$x(k) = \left[x_{k1} \quad x_{k2} \quad \cdots \quad x_{kn} \quad \cdots \quad x_{kN}\right]^T$$

The vectors $\underline{f}$ and $\underline{x}$ and the matrix ϕ^T can be written in terms of their elements as

$$\begin{aligned} f_1 &= \phi_{11,1}x_{11} + \phi_{12,1}x_{12} + \ldots + \phi_{kn,1}x_{kn} + \ldots + \phi_{MN,1}x_{MN} \\ f_2 &= \phi_{11,2}x_{11} + \phi_{12,2}x_{12} + \ldots + \phi_{kn,2}x_{kn} + \ldots + \phi_{MN,2}x_{MN} \\ &\vdots \\ f_q &= \phi_{11,q}x_{11} + \phi_{12,q}x_{12} + \ldots + \phi_{kn,q}x_{kn} + \ldots + \phi_{MN,q}x_{MN} \\ &\vdots \\ f_{p^2} &= \phi_{11,p^2}x_{11} + \phi_{12,p^2}x_{12} + \ldots + \phi_{kn,p^2}x_{kn} + \ldots + \phi_{MN,p^2}x_{MN} \end{aligned} \qquad (9)$$

Substitute $\underline{f}$ from (8) into (3) and the result becomes

$$\begin{aligned} \underline{y} &= \phi\phi^T \underline{x} \\ \underline{y} &= G\underline{x} \qquad \text{where} \quad G = \phi\phi^T \end{aligned} \qquad (10)$$

G is the natural pixels matrix. As can be seen from (10), the element G_{ij} is a correlation between the i^{th} and the j^{th} strips. And the component y_i of the projection vector $\underline{y}$ is the summation of all contribution of each correlation between the i^{th} and the j^{th} strips, starting from j = 1 to MN.

4.1 The effects of number of pixels

In this study we evaluate the effects of the number of pixels from the values of the vector $\underline{x}$ in (8). Since the test function $\underline{f}$ is known, $\underline{x}$ can be determined directly from

$$\underline{x} = (\phi^T)^{-1}\underline{f}$$

Since the problem is over-determined, the singular value decomposition technique is used to solve the above equation. Evaluation of $\underline{x}$ directly from this method rather than that from the reconstruction result, has an advantage in that the reconstruction errors can be avoided, thanks to the computer simulated test function $\underline{f}$.

The solutions $\underline{x}$ are obtained for the different numbers of p^2 (= 32 x 32, 64 x 64, and 128 x 128 pixels) but a fixed number of MN (8 angles x 64 strips). Since the solutions $\underline{x}$ do not have a physical meaning, we then interpret the solutions in terms of the approximation functions of $\underline{f}$. Using the solutions $\underline{x}$, three different approximation functions of $\underline{f}$ are shown in Figure 3

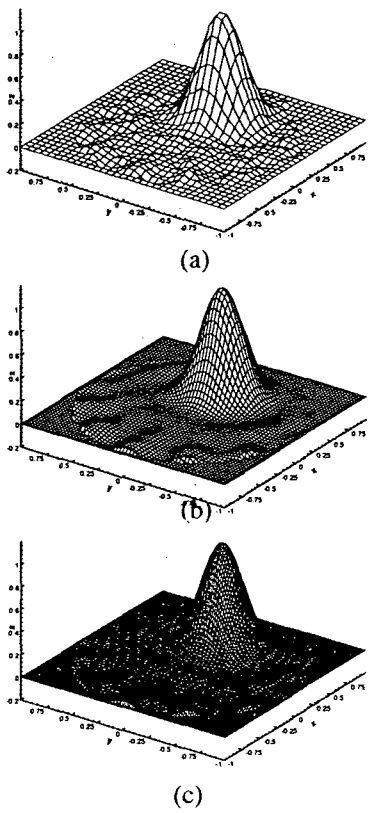

Figure 3 Approximation function $\underline{f}$ (a) 32 x 32 pixels (b) 64 x 64 pixels (c) 128 x 128 pixels

It is shown in Figures 3a to 3c that a similar streakline pattern appears on all of the approximation functions. Increasing the number of pixels does not overcome the streakline error. This is due to the fact that the number of projection strips of the matrix ϕ^T, both lateral and angular, is limited to MN (8x64 strips).

4.2 The effects of number of projections

The accuracy of the lateral strip projections is studied by comparing the strips obtained from (3) with that from analytical integration of (2). The calculation of projection strips from (3) is straightforward while the analytical strip projection of the particular test function can be obtained by

$$p_s(r_i) = \int_{r_i-\frac{1}{2}}^{r_i+\frac{1}{2}} p_\theta(r)dr = \int_{r_i-\frac{1}{2}}^{r_i+\frac{1}{2}} \sqrt{\frac{\pi}{c}} e^{-c(r-R)^2} dr \qquad (11)$$

where $R = \sqrt{x_0^2 + y_0^2}\cos\left\{\left[\tan^{-1}\left(\frac{y_0}{x_0}\right)\right] - \theta\right\}$

Figure 4 compares the strip projection functions between those obtained from discrete projections, (3), and those from direct integration, (11). The results are calculated for different values of strips per view angle (32, 64 and 128 strips) but a fixed number of pixels (64 x 64 pixels). Errors are presented as percentage of root-mean-square error. The error decreases, noticeably, when the number of strips increases from 32 to 64 but negligibly when the number of the strips increases from 64 to 128. This demonstrates that the accuracy of the projection strips has reached its limit for the given number of pixels.

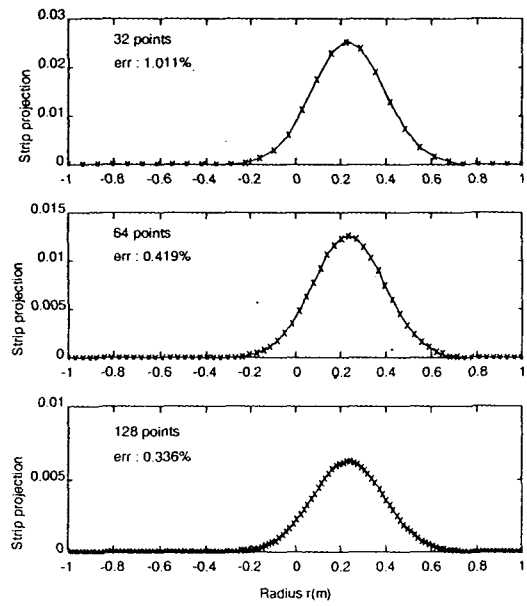

Figure 4 Projection function : direct integrated (solid line),

4.3 The effects of number of view angles

Effects of the number of angular samplings are shown by Figure 5. The Figure is obtained by calculating the approximation function of f, using the solutions of $\underline{x}$ for different number of angular views (4, 8, and 16 view angles) but for a fixed number of pixels (p^2 = 64 x 64) and lateral projection strips (64 strips per angular view). It is clearly demonstrates that for the given numbers of the pixels and the lateral projection strips, a more accurate approximation function f is obtained when more angular samplings are used.

5. Reconstruction Results

It has been shown from the previous section that an appropriate dimension of the projection matrix ϕ affects the accuracy of the unknown coefficient vector $\underline{x}$. In this paper, the projection matrix ϕ is constructed based on 64 x 64 pixels, 64 strips for each angular view. The number of angular sampling is

left as unknown, which is usually the case for combustion measurement.

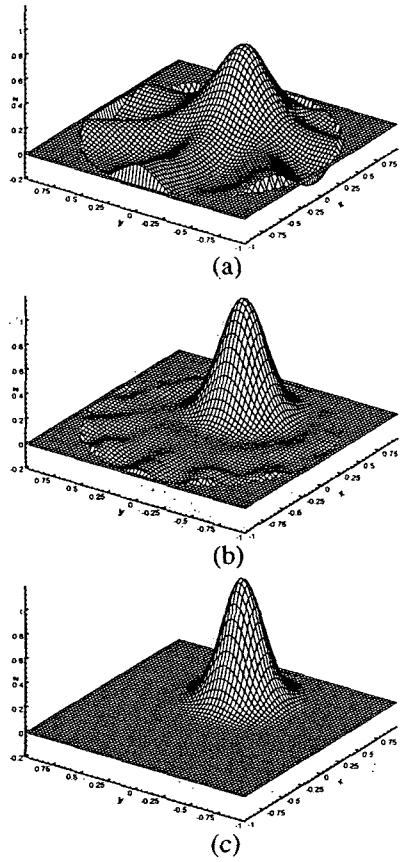

Figure5 Approximation function f : (a) 4 sampling angles (b) 8 sampling angles (c) 16 sampling angles

Figure 6 shows the reconstruction results of the test function from their analytical path-integrated data. Three reconstruction techniques are used: FBP, ART and NP techniques. Picture distance (PD) measure as we used in our previous work [3] is again used to evaluate the resemblance of the reconstruction results to the test function.

It is shown from Figure 6 that the ART and NP techniques give a better reconstruction result than FBP. The results of FBP and ART are comparable when the higher number of angular views are used. Figures 7 to 9 show the surface plots of the reconstructed functions by using FBP, ART and NP techniques respectively. Consider particularly the NP result, it is shown in Figure 9 that the PD measure is high compared to the other techniques when higher angular views are used and the error smears over the entire region, which is similar to white noise. Improving the matrix-inversions technique using an appropriate technique, e.g. wavelets, is under way in the current series of investigations.

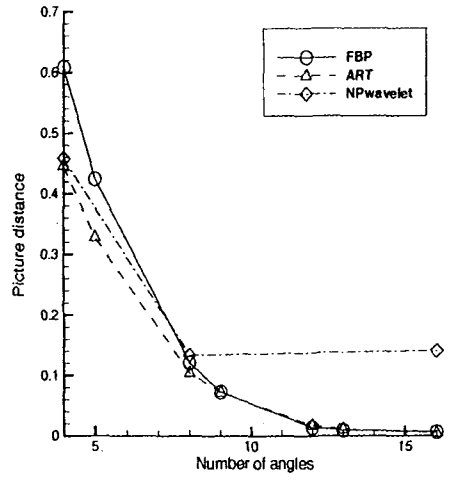

Figure 6 Picture distance : FBP, ART and NP.

6. Conclusions

Discrete tomographic reconstruction of an off-centered Gaussian function from its incomplete data has been studied. With this method, the Gaussian function is assumed to be a discrete function at the beginning of the reconstruction process. A projection matrix, which projects the test function into projection strips, is constructed and its characteristics studied. It is shown from the study that the accuracy of the reconstruction result depends mainly on an appropriate dimension of the projection matrix. Reconstruction results using the FBP, ART and NP techniques have been studied and compared. It is found that when a small number of view angles (less than 8) is used the ART and NP techniques give more accurate reconstruction results than the FBP. On the other hand, when a large number of view angles is used the reconstruction results using the ART and FBP are in good agreement with the test function. There appears to be a white noise pattern in the reconstruction results when using the NP technique with a large number of angular samplings. To solve this problem, an advanced algorithm for the solution of a large matrix is needed.

Acknowledgement

This work was supported in part by The Thailand Research Fund , Grant No. PDF/53/2540.

References

[1]. Nyden, M.R. ; Vallikul, P. ; and Sivathanu, Y.R., Journal of Quantitative Spectroscopy & Radiative Transfer 55 No. 3 (1996) : 345-356.

[2]. Sivathanu, Y.R. , and Gore, J.P.,Journal of Quantitative Spectroscopy & Radiative Transfer 50 (1993) : 483

[3]. Vallikul, P. ; Goulard, R. ; Mavriplis, C. ; and Nyden, M.R. "Tomographic Reconstruction of Probability Density Functions in Turbulent Flames." Conference Proceedings of The Seventh International Fire Science and Engineering Conference (Interflame'96), St. John's College, Cambridge, England, 26-28 March 1996 : 235-243

[4]. Shepp, L.A. , and Logan, B.F.,IEEE Transection on Nuclear Science NS-21 (1974) : 21

[5]. Chapman C.H. , and Cary P.W. ,Inverse Problem 2 (1986) : 23-49

[6]. Buonocore, M.H. ; Brody, W.R. ; and Macovski, A. IEEE Transactions on Biomedical Engineering Vol. BME-28 No. 2 (February 1981) : 69-78.

[7]. Beiting, E.J. , Optics Letters 16 (1991) : 1281.

[8]. Rosenfeld, A. , and Kak, A.C. Digital Picture Processing 2 nd ed. New York : Academic Press, 1982.

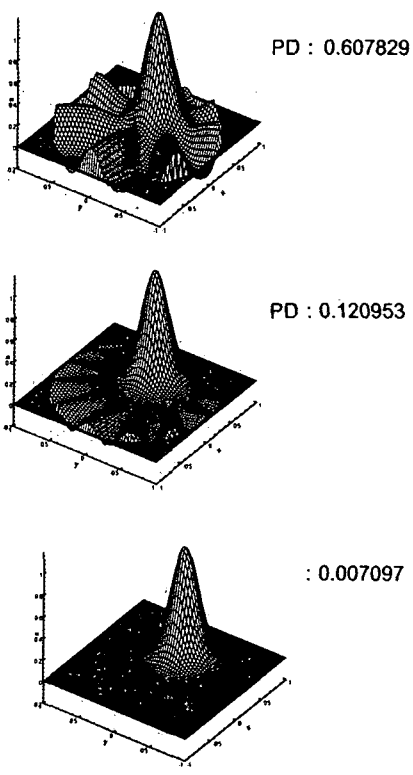

Figure 7 Reconstruction results using FBP technique with 4 ,8 and 16 sampling angles respectively

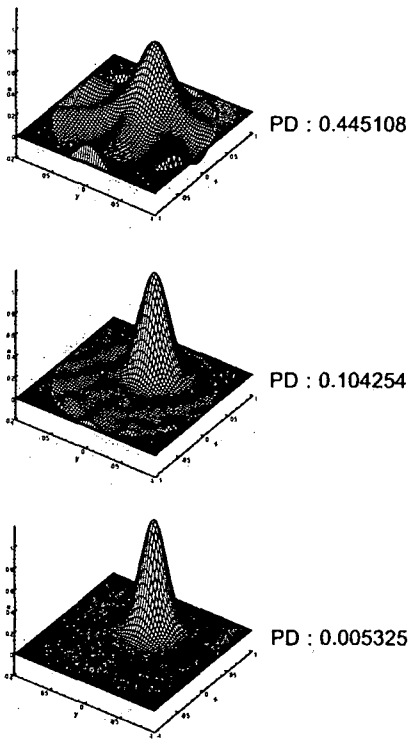

Figure 8 Reconstruction results using ART technique with 64 sampling points (a) 4 sampling angles (b) 8 sampling angles (c) 16 sampling angles

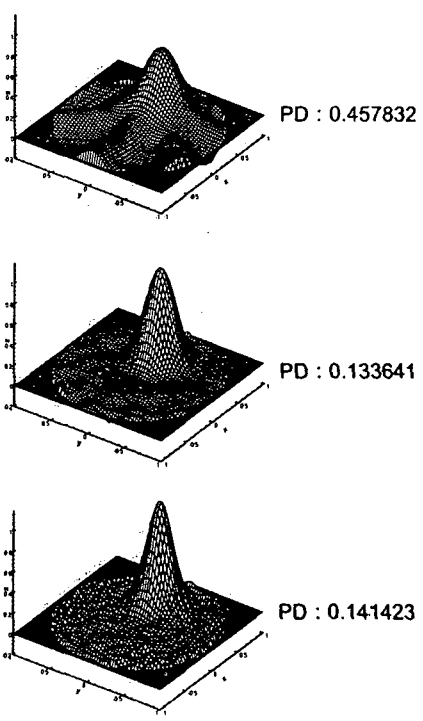

Figure 9 Reconstruction results using wavelet-NP technique with 4,8 and 16 sampling angles respectively